Proc. Natl. Acad. Sci. USA
Vol. 96, pp. 4662–4667, April 1999
Neurobiology

An apamin-sensitive Ca^{2+}-activated K^+ current in hippocampal pyramidal neurons

MARTIN STOCKER, MICHAEL KRAUSE, AND PAOLA PEDARZANI*

Max Planck Institute for Experimental Medicine, Department of Molecular Biology of Neuronal Signals, 37075 Göttingen, Germany

Communicated by Per O. Andersen, University of Oslo, Oslo, Norway, January 29, 1999 (received for review November 19, 1998)

ABSTRACT **In hippocampal and other cortical neurons, action potentials are followed by afterhyperpolarizations (AHPs) generated by the activation of small-conductance Ca^{2+}-activated K^+ channels (SK channels). By shaping the neuronal firing pattern, these AHPs contribute to the regulation of excitability and to the encoding function of neurons. Here we report that CA1 pyramidal neurons express an AHP current that is suppressed by apamin and is involved in the control of repetitive firing. This current presents distinct kinetic and pharmacological features, and it is modulated differently than the apamin-insensitive slow AHP current. Furthermore, our *in situ* hybridizations show that the apamin-sensitive SK subunits are expressed in CA1 pyramidal neurons, providing a potential molecular correlate to the apamin-sensitive AHP current. Altogether, these results clarify the discrepancy between the reported high density of apamin-binding sites in the CA1 region and the apparent lack of an apamin-sensitive current in CA1 pyramidal neurons, and they may explain the effects of this toxin on hippocampal synaptic plasticity and learning.**

In many neurons of the central nervous system, action potentials are followed by a rise in intracellular Ca^{2+} leading to a prolonged afterhyperpolarization (AHP) of the membrane (1–4). The currents underlying the AHP are mediated by small-conductance voltage-insensitive Ca^{2+}-activated K^+ channels (SK channels), and they can be classified into two groups on the basis of their kinetic and pharmacological properties (5): (*i*) I_{AHP} is sensitive to the bee venom toxin apamin and presents a relatively fast activation and decay (6); (*ii*) sI_{AHP} (where *s* stands for *s*low) is apamin insensitive, rises to peak and decays with time constants of several hundreds of milliseconds, and is modulated by many neurotransmitters (1, 4). Functionally, activation of I_{AHP} controls the firing frequency in tonically spiking neurons, whereas activation of sI_{AHP} leads to spike frequency adaptation (5). While most excitable cells present an apamin-sensitive I_{AHP}, only a few nerve cells exhibit an apamin-insensitive sI_{AHP}, or both types of currents (4, 5). In the hippocampus, electrophysiological experiments have so far shown a peculiar segregation of AHP currents in different types of neurons, with pyramidal neurons presenting exclusively sI_{AHP} (1, 7), and oriens–alveus interneurons only I_{AHP} (8). These results are in contrast with studies on the distribution of apamin-binding sites in rat brain sections, which show the highest density in the hippocampal CA1 region (9, 10).

Three members of the SK family of K^+ channels have recently been cloned (11). All of them are voltage-insensitive and activated by submicromolar intracellular Ca^{2+}. Two of them, SK2 and SK3, are blocked by apamin, whereas SK1 is apamin insensitive (11). Given these features, the SK channel subunits cloned so far are likely to participate in the formation of native SK channels, giving rise to apamin-sensitive and -insensitive AHP currents in different neurons.

In this study, we have used a combination of electrophysiological and pharmacological tools to reveal the presence of an apamin-sensitive AHP current, I_{AHP}, in CA1 pyramidal neurons, and we have demonstrated by *in situ* hybridization that the apamin-sensitive SK subunits potentially underlying this current are highly expressed in these cells. These results reconcile the discrepancy between the high density of binding sites for apamin detected in the CA1 layer (9, 10) and the apparent lack of apamin-sensitive currents in CA1 pyramidal neurons (1, 7). The apamin-sensitive I_{AHP} characterized here presents a different modulation profile by neurotransmitters in comparison with sI_{AHP}, and it seems to play a role in the control of repetitive firing and in the regulation of excitability of CA1 pyramidal neurons.

METHODS

***In Situ* Hybridization.** *In situ* hybridization was performed on brain sections (10–16 μm) from male rats by using ^{35}S-labeled antisense and sense oligonucleotide probes according to the procedure described in detail in ref. 12. For each SK channel subunit, at least two antisense oligonucleotides corresponding to the 5′ and 3′ regions with no significant similarity to the other known SK channel subunits were chosen (SK1, 5′-GGCCTGCAGCTCCGACACCACCTCATATGCGATGCTCTGTGCCTT-3′ and 5′-CAGTGGCTTTGTGGGCTCTGGGCGGCTGTGGTCAGGTGACTGGGC-3′; SK2, 5′-AGCGCCAGGTTGTTAGAATTGTTGTGCTCCGGCTTAGACACCACG-3′ and 5′-CTTCTTTTTGCTGGACTTAGTGCCGCTGCTGCTGCCATGCCCGCT-3′; and SK3, 5′-CGATGAGCAGGGGCAGGGAATTGAAGCTGGCTGTGAGGTGCTCCA-3′ and 5′-TAGCGTTGGGGTGATGGAGCAGAGTCTGGTGGGCATGGTTATCCT-3′). The sense oligonucleotides had sequences complementary to the second oligonucleotide listed for each channel, and they were used to control for general background on adjacent sections. Specificity of the observed signals was confirmed in three ways: (*i*) identical hybridization patterns were obtained with each pair of antisense oligonucleotides; (*ii*) hybridization with a mixture of the same labeled and nonlabeled oligonucleotide in 100- to 500-fold excess did not result in detectable signal (Fig. 1D); and (*iii*) a mixture of labeled oligonucleotide specific for a certain SK subunit and nonlabeled oligonucleotides for other SK subunits resulted in the same hybridization pattern as obtained with the specific antisense oligonucleotide alone. Specimens were exposed to Kodak Biomax x-ray film for 8–14 days. For cellular resolution, selected slides were dipped

Abbreviations: AHP, afterhyperpolarization; I_{AHP}, afterhyperpolarizing current; sI_{AHP}, slow I_{AHP}; SK channels, small-conductance voltage-insensitive Ca^{2+}-activated K^+ channels; 8CPT-cAMP, 8-(4-chlorophenylthio)adenosine 3′,5′-cyclic monophosphate.

*To whom reprint requests should be addressed at: Max Planck Institute for Experimental Medicine, Dept. Molecular Biology of Neuronal Signals, Hermann-Rein-Str. 3, 37075 Göttingen, Germany. e-mail: pedarzani@mail.mpiem.gwdg.de.

The publication costs of this article were defrayed in part by page charge payment. This article must therefore be hereby marked "*advertisement*" in accordance with 18 U.S.C. §1734 solely to indicate this fact.

PNAS is available online at www.pnas.org.

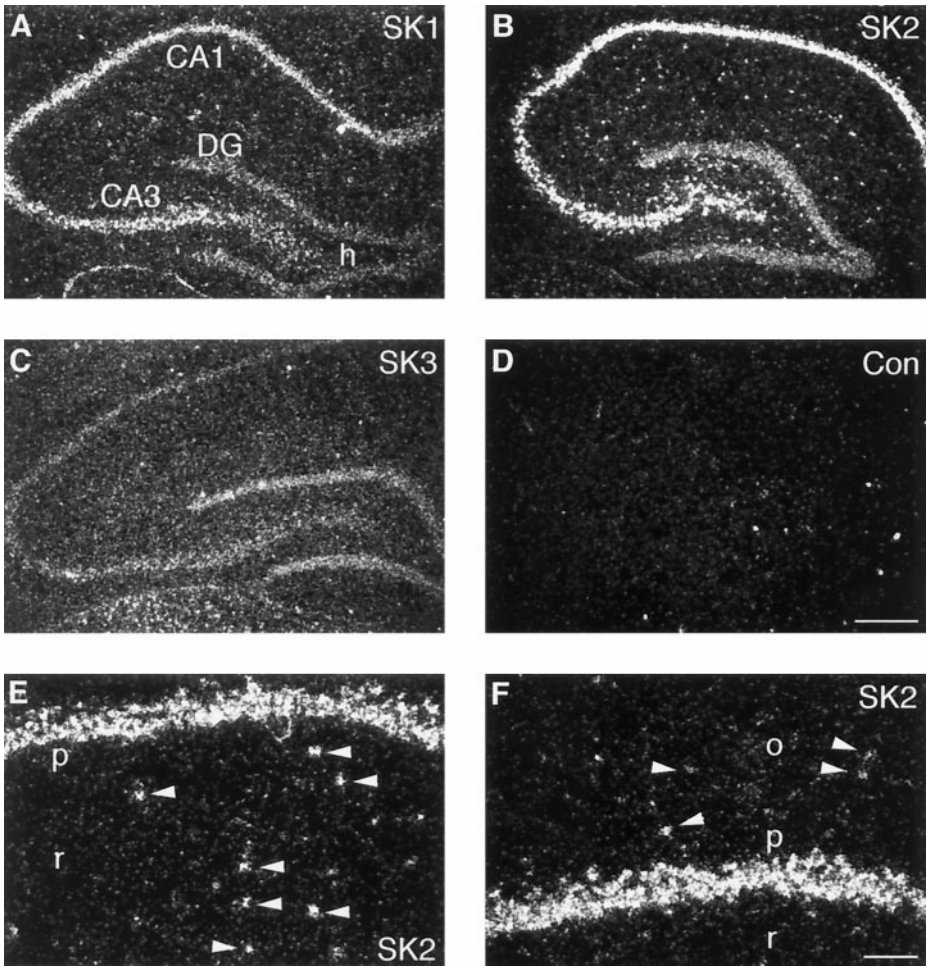

FIG. 1. Dark-field photomicrographs of sagittal and coronal sections through the rat hippocampal region hybridized with oligonucleotides specific for SK1 (*A*), SK2 (*B*), and SK3 (*C*) and control (*D*). (*E* and *F*) High magnification of the CA1 region, showing expression of SK2 in pyramidal neurons and in interneurons (arrowheads) in stratum radiatum (*E*) and in stratum oriens (*F*). CA1, CA3, pyramidal cell layer of the CA1 and CA3 fields; DG, granule cell layer of the dentate gyrus; h, hilus proper; p, CA1 pyramidal cell layer; r, stratum radiatum; o, stratum oriens. (Scale bars: *A–D,* 400 μm; *E* and *F*, 100 μm.)

in photographic emulsion Kodak NTB2 and developed after 12–20 weeks. Congruent data were provided by x-ray film images and emulsion-dipped slides. Brain structures were identified according to ref. 13.

Electrophysiology and Pharmacology. Transverse hippocampal slices (300 μm thick) were prepared from young Wistar rats (18–30 days old) as described (14). During recording, the slices were superfused with standard artificial cerebrospinal fluid (ACSF) containing (mM): 125 NaCl, 25 $NaHCO_3$, 1.25 KCl, 1.25 KH_2PO_4, 2.5 $CaCl_2$, 1.5 $MgCl_2$, and 16 glucose, saturated with 95% O_2 and 5% CO_2, at room temperature (21–24°C). In voltage-clamp experiments tetrodotoxin (TTX; 0.5 μM) and tetraethylammonium (TEA; 1 mM) were added to the ACSF. Whole-cell gigaseal recordings were obtained from CA1 pyramidal cells in the slice by using the "blind" method (15). The patch pipette solution contained (mM): 135 potassium gluconate, 10 KCl, 10 Hepes, 2 Na_2ATP, 1 $MgCl_2$, and 0.4 Na_3GTP (pipette resistance: 3–6 MΩ); 8-(4-chlorophenylthio)adenosine 3′,5′-cyclic monophosphate (8CPT-cAMP; 50 μM) was included to measure the apamin-sensitive AHP current in isolation. All neurons included in this study had a resting membrane potential below −55 mV (−62 ± 1 mV; $n = 55$) and an input resistance of 218 ± 5 MΩ ($n = 55$). Using an EPC-9 amplifier (HEKA Electronics, Lambrecht/Pfalz, Germany), we voltage-clamped cells at −50 mV and, once every 30 s, applied depolarizing steps (100 ms long) of sufficient amplitude (typically +60 to +70 mV) to elicit a robust, unclamped Ca^{2+} action current. The access resistance (range 10–25 MΩ) and the amplitude and time course of the Ca^{2+} current during the step showed only minimal variations during the recordings included in this study. Only cells with a stable resting potential throughout the current-clamp protocols (±0.5 mV) were included in the analysis. Records were filtered at 0.25–1 kHz and digitized at 1–4 kHz. All data were acquired, stored, and analyzed on a Power Macintosh 7100/66 using the PULSE+PULSEFIT software (HEKA Electronics) and IGOR PRO (WaveMetrics, Lake Oswego, OR). Values are reported as mean ± SEM. Student *t* test was used for statistical comparisons between groups ($\alpha = 0.05$).

RESULTS AND DISCUSSION

As a first approach to the molecular identification of SK channels in hippocampal neurons, we studied the expression of SK1, SK2, and SK3 mRNA by *in situ* hybridization with oligonucleotide probes. Examination of x-ray film images revealed that all three subunits are present in the rat hippocampus, displaying different expression patterns and abundance. These data are in agreement with overview autoradiograms obtained with RNA probes (11). Analysis at cellular resolution showed that the transcript for the apamin-insensitive SK1 subunit was present at moderate levels in pyramidal cells of the CA1 to CA3 region, whereas granule cells in the dentate gyrus displayed a low level of SK1 mRNA

(Fig. 1*A*). The SK3 subunit was expressed at low levels in the pyramidal cell layer of the CA1 to CA3 fields, being slightly elevated in dentate gyrus granule cells (Fig. 1*C*). By contrast, the SK2 transcript was strongly expressed by CA1–CA3 pyramidal neurons as well as interneurons scattered in stratum radiatum and oriens and in the dentate gyrus hilus (Fig. 1 *B*, *E*, and *F*) but was slightly less abundant in dentate gyrus granule cells (Fig. 1*B*). The predominance of the apamin-sensitive SK2 subunit in stratum oriens interneurons fits with electrophysiological data on the presence of an apamin-sensitive AHP current in these cells (8). On the contrary, the high expression of SK2 subunits in pyramidal neurons of the CA1 and CA3 regions is not corroborated by electrophysiological evidence, since the AHP current has been reported to be apamin insensitive in these cells (1, 7). We therefore decided to test whether an apamin-sensitive AHP current is present in these neurons.

It has recently been reported that bicuculline, a blocker of the γ-aminobutyrate (GABA) type A receptor, suppresses an apamin-sensitive AHP current in midbrain and thalamic neurons at concentrations commonly used to block inhibitory synaptic transmission (16–18). We investigated the effect of this compound on the AHP current in CA1 pyramidal neurons. The current was elicited as a tail current following an unclamped Ca^{2+} current produced by a short depolarizing pulse, in the presence of tetrodotoxin (0.5 μM) to block Na^+ channels (14). Bicuculline methochloride (10 μM) selectively and reversibly suppressed a faster current preceding and partially overlapping with the slow AHP current, sI_{AHP}, but had no effect on sI_{AHP} itself (Fig. 2*A*; $n = 5$). The suppression of the faster component might explain why in previous studies in which bicuculline was used, this current was not detected (14). Another substantial difference from previous work in which the bicuculline-sensitive current was not reported (1, 19) resides in the use of the whole-cell technique with a relatively low and stable access resistance.

In the rest of this study, we characterized the current revealed in the absence of bicuculline and tested whether it corresponded to the voltage-independent, Ca^{2+}-activated apamin-sensitive AHP current, I_{AHP}. Whole-cell recordings were obtained from 134 CA1 pyramidal neurons in rat hippocampal slices. The bicuculline-sensitive current showed a fast exponential decay with a time constant of 89 ± 4 ms (Fig. 2*B*, left; $n = 30$), and no voltage dependence. A similar time course (76 ± 6 ms; $n = 18$) was estimated in the absence of 8CPT-cAMP, thereby excluding a possible effect of this compound on the time course of this current. Compared with the 30-fold slower sI_{AHP} (Fig. 2*B*, *Right*; decay time constant: 2,800 ± 100 ms; $n = 17$), and to the 5-fold faster I_C, underlying the fast AHP and presumably mediated by high conductance Ca^{2+}-activated K^+ channels [BK; (4)], the bicuculline-sensitive current presented a time course of intermediate duration (medium current). In all cells measured the medium current coexisted with sI_{AHP}, had a larger peak amplitude (medium current, 120 ± 8 pA; sI_{AHP}, 54 ± 5 pA; $n = 19$), but the relative sizes of the two currents varied from cell to cell (medium current/sI_{AHP} ratio ranged from 1.3 to 3.7). This observation, together with the pharmacological separation by bicuculline, suggests that they are independent currents. To characterize the properties of the medium current in isolation, we included the cAMP analogue 8CPT-cAMP in the pipette solution to suppress sI_{AHP} (14) (Fig. 2*B Left*). The reversal potential of the medium current measured in isolation was −95 ± 3 mV ($n = 5$), fairly close to −101 mV, the value predicted by the Nernst equation for a K^+-selective conductance.

Superfusion with Ca^{2+}-free solution led to a reversible suppression of both medium current and sI_{AHP} (Fig. 2*E*), or of the medium current elicited in isolation (Fig. 2 *C* and *E*). Similar results were obtained for both currents with the Ca^{2+} channel blocker Cd^{2+} (50–200 μM; Fig. 2 *D* and *E*), indicating that influx of extracellular Ca^{2+} is necessary for their activation.

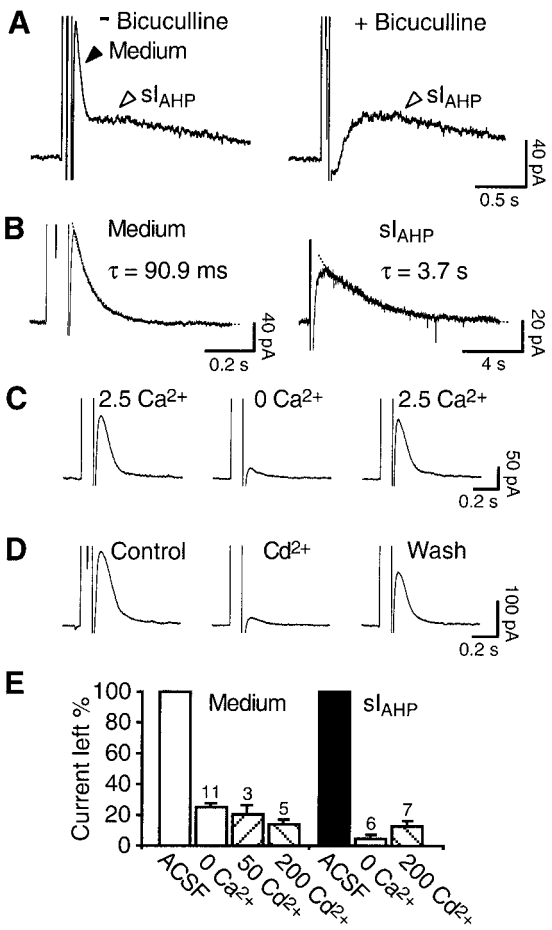

FIG. 2. Whole-cell recordings showing two distinct voltage-independent Ca^{2+}-activated currents in CA1 pyramidal neurons. (*A*) In the absence of bicuculline (*Left*), a 100-ms depolarizing pulse to +10 mV in the presence of tetrodotoxin (0.5 μM) and tetraethylammonium (1 mM) elicits two distinct currents. In the presence of bicuculline (10 μM), the medium current (Medium) is blocked, whereas the slow AHP current, sI_{AHP}, persists unaffected (*Right*). (*B*) Representative example of the medium current measured in isolation after suppression of sI_{AHP} by intracellular application of 8CPT-cAMP (50 μM; *Left*), in comparison with sI_{AHP} measured in the presence of apamin (50 nM; *Right*). The decay time courses of both currents were fitted by mono-exponential functions (dotted lines). (*C*) The medium current is reversibly suppressed in nominally Ca^{2+}-free ACSF containing 5 mM Mg^{2+}. (*D*) The Ca^{2+} channel blocker Cd^{2+} (50 μM) produces a partially reversible suppression of the medium current. (*E*) Bar diagram summarizing the effects of Ca^{2+}-free medium and Cd^{2+} (50–200 μM) on the medium current (left four bars) and sI_{AHP} (right three bars). Numbers of experiments are reported over the corresponding bars.

These results suggest that the medium current reversibly blocked by bicuculline is indeed a voltage-independent, Ca^{2+}-dependent K^+ current, presenting kinetic features distinct from those of the well characterized sI_{AHP} in CA1 pyramidal neurons.

We next tested whether the bicuculline-sensitive medium current is blocked by the specific SK channel toxins apamin and scyllatoxin in CA1 pyramidal neurons. Apamin suppressed the medium current, when measured in the presence or in the absence of sI_{AHP} (Fig. 3 *A* and *B*). As previously shown (1), apamin concentrations up to 200 nM did not affect sI_{AHP} (Fig. 3*A Right* and *F*). The concentration of apamin producing a half-maximal suppression of the medium current (IC_{50}) was ≈480 pM (Fig. 3*C*). The scorpion toxin scyllatoxin blocks

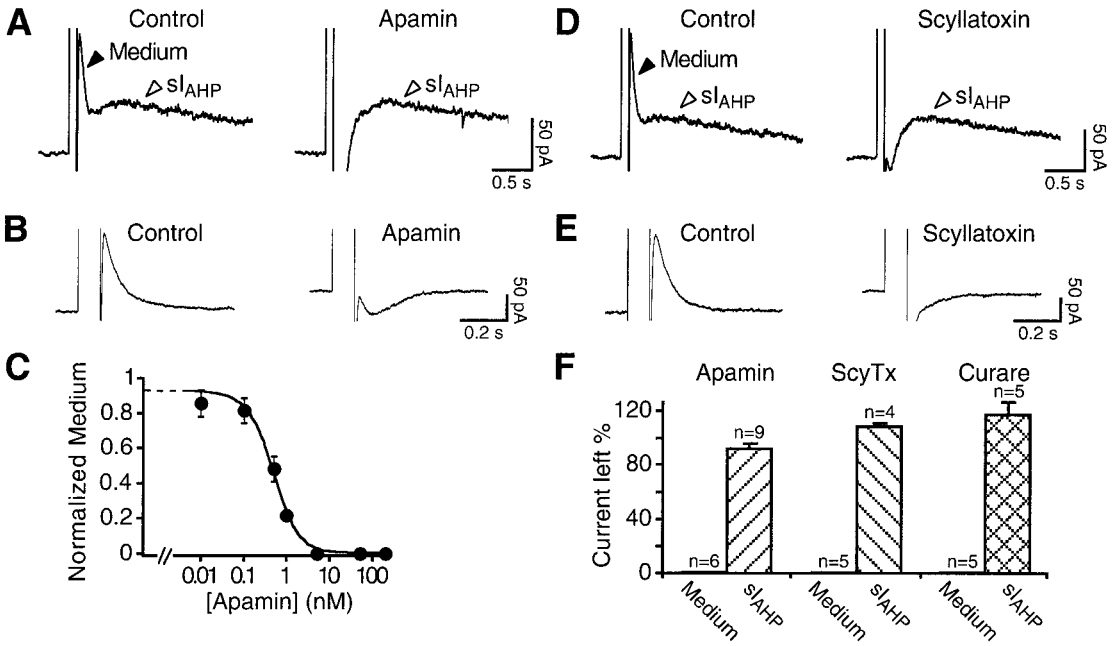

FIG. 3. Pharmacological characterization of the bicuculline-sensitive current. At 50 nM, apamin (*A*) and scyllatoxin (*D*) selectively block the medium current and do not affect sI_{AHP}. The block of the medium current uncovers a Ca^{2+}-dependent inward current. Similarly, in *B* apamin (50 nM) and in *E* scyllatoxin (50 nM) block the medium current measured in isolation in the presence of 8CPT-cAMP. (*C*) Dose–response curve for the block of the medium current by apamin. Data points were fit with a Langmuir isotherm, giving an IC_{50} value of ≈480 pM and a Hill coefficient of 0.92. For each point $n = 3$–7; error bars are SEM. (*F*) Bar diagram summarizing the effects of apamin (50 nM), scyllatoxin (ScyTx; 50 nM), and tubocurarine (curare; 50 μM) on the medium current and sI_{AHP}.

apamin-sensitive SK channels in hepatocytes and muscle cells, and its receptors colocalize with the apamin-binding sites in the central nervous system (20–23). Similarly to apamin, scyllatoxin (50 nM) suppressed selectively the medium current, without affecting sI_{AHP} in CA1 neurons (Fig. 3 *D* and *F*). In Fig. 3*E*, the effect of scyllatoxin is shown on the isolated medium current. This is, to our knowledge, the first functional demonstration that the target of this toxin is the same channels as those blocked by apamin in the mammalian central nervous system. Neither the effect of apamin nor that of scyllatoxin was reversible. Finally, we tested the nicotinic acetylcholine receptor blocker tubocurarine, known to block apamin-sensitive SK channels in a variety of neuronal and nonneuronal cells (24–27). Tubocurarine (50 μM; $n = 5$) suppressed in a reversible way the putative I_{AHP}, without affecting sI_{AHP} (Fig. 3*F*). Neither charybdotoxin (100 nM) nor iberiotoxin (50 nM) or tetraethylammonium at low concentrations (1 mM), all blocking high-conductance Ca^{2+}-activated K^+ channels (BK), affected the medium current or sI_{AHP} (not shown). The characteristic pharmacological profile of the medium current adds a further line of evidence to the molecular and electrophysiological data strongly supporting the presence of a kinetically and pharmacologically distinct apamin-sensitive I_{AHP} in CA1 pyramidal neurons.

A characteristic feature of sI_{AHP} is its modulation by a large number of neurotransmitters, leading to a reduction in spike frequency adaptation and to an increased excitability of hippocampal and other cortical neurons (5, 28). By contrast, no direct modulation of the apamin-sensitive I_{AHP} has so far been reported in neurons of the mammalian central nervous system (6, 29). We tested whether in CA1 pyramidal neurons I_{AHP} is modulated. Application of the β-adrenergic receptor agonist isoproterenol, acting by means of cAMP–protein kinase A, led to a complete suppression of sI_{AHP}, as expected (Fig. 4 *A* and *D*; see also ref. 14). By contrast, the peak amplitude of I_{AHP} was significantly increased by approximately 20% in all cells tested (range: 7.2–31.5%; $P = 0.015$; Fig. 4 *A* and *D*). This effect was partly mimicked by the membrane-permeant cAMP analogue 8CPT-cAMP applied to the bath in 3 of 4 cells (range: 5.3–12%; $P = 0.045$; Fig. 4*D*). The current enhanced by isoproterenol or 8CPT-cAMP displayed a time course indistinguishable from the control, and an unchanged sensitivity to apamin ($n = 8$; not shown). The cholinergic agonist carbachol, acting through muscarinic receptors, produced a suppression of sI_{AHP} and a small reduction of I_{AHP} (Fig. 4 *B* and *D*). A quantification of the observed effects on I_{AHP} amplitude is nevertheless difficult, because (*i*) I_{AHP} and sI_{AHP} are partially overlapping, to an extent variable from cell to cell (Fig. 4*C*), leading to a possible decrease in I_{AHP} amplitude as a consequence of sI_{AHP} suppression, and (*ii*) I_{AHP} and sI_{AHP} are likely to be partly counterbalanced by an inward current. Thus, blockade of I_{AHP} and sI_{AHP} disclosed a Ca^{2+}-dependent inward current (Fig. 3 *A, B, D,* and *E*), most likely mediated by nonselective cationic channels (30, 31). These results suggest that neurotransmitters acting via the cAMP–protein kinase A pathway might differentially modulate sI_{AHP} and I_{AHP} in CA1 neurons, producing a suppression of the former and a small, but consistent, enhancement of the latter current, as in the case of isoproterenol. By contrast, neurotransmitters acting via other pathways, such as cholinergic agonists, seem to affect selectively sI_{AHP}, with little or no effect on I_{AHP}. Further work is needed to better quantify the effect of monoamines on I_{AHP} and on the counterbalancing inward current and to elucidate the underlying mechanism.

To investigate the functional role of the apamin-sensitive I_{AHP}, we performed current-clamp recordings. In hippocampal pyramidal cells, bursts of action potentials are followed by two AHPs: a medium AHP (mAHP) lasting 50–100 ms (7), and a slow AHP (sAHP) lasting several seconds (4, 5). In the presence of bicuculline, two potassium currents have been suggested to mainly contribute to the mAHP: the voltage-dependent I_M and the voltage- and Ca^{2+}-dependent I_C (7). In the absence of bicuculline, apamin (50 nM) reduced the mAHP (Fig. 5*A*, filled arrowhead; $n = 5$), without significantly affecting the resting membrane potential and the sAHP (Fig. 5*A*, open arrowhead). Furthermore, it produced a small increase in

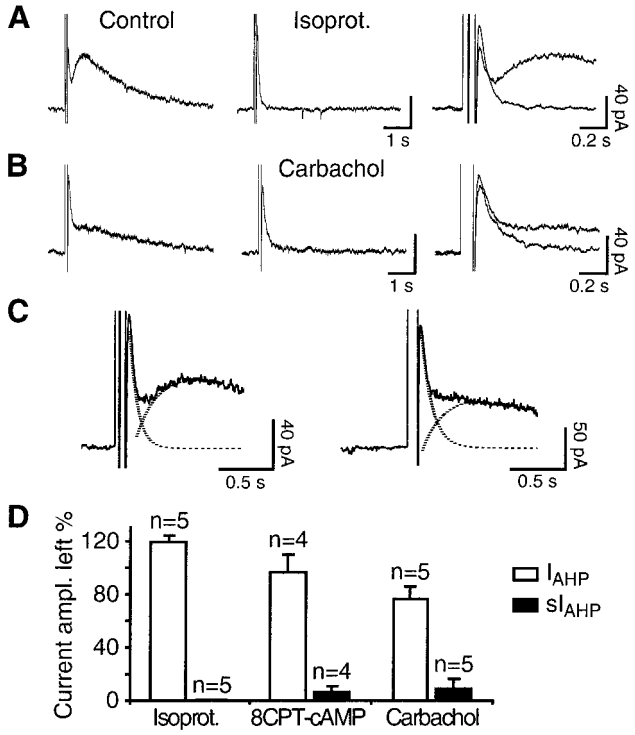

FIG. 4. Differential modulation of I_{AHP} and sI_{AHP} by neurotransmitters and second messengers. (*A*) The β-adrenergic receptor agonist isoproterenol (0.5 μM) suppresses completely sI_{AHP} and increases I_{AHP}. (*B*) The cholinergic agonist carbachol (2.5 μM) inhibits sI_{AHP} and produces a small decrease in I_{AHP} peak amplitude. On the right, the traces are displayed expanded and superimposed. (*C*) The decay of I_{AHP} and the rise time of sI_{AHP}, measured in the same cell in the presence of apamin, were fitted with monoexponential functions (dashed lines) and overlap to an extent variable from cell to cell: small overlap (*Left*), big overlap (*Right*). Depending on the degree of overlap, a suppression of sI_{AHP} would produce an apparent decrease in I_{AHP} peak amplitude. (*D*) Bar diagram summarizing the effects of isoproterenol, 8CPT-cAMP, and carbachol on I_{AHP} and sI_{AHP}.

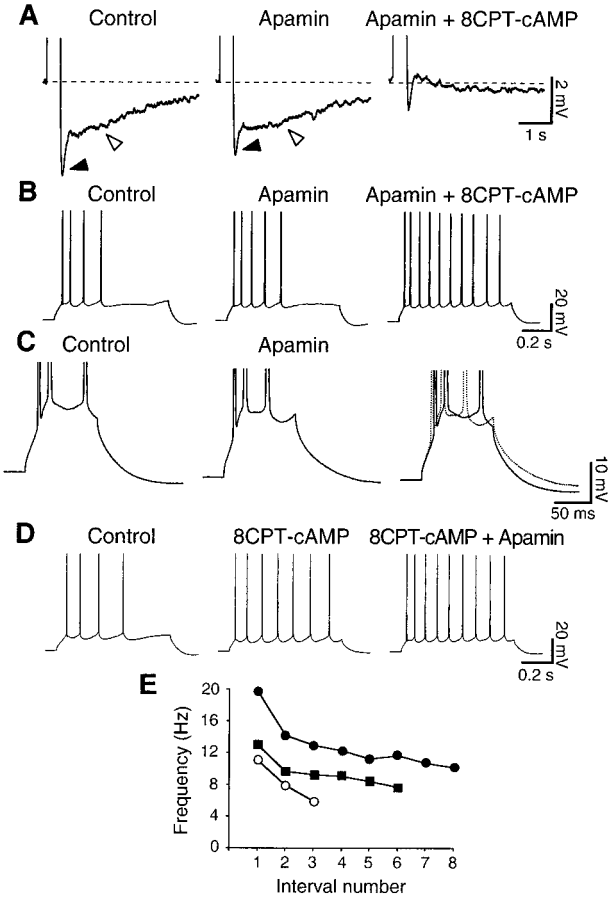

FIG. 5. The apamin-sensitive AHP plays a role in controlling the firing properties of CA1 pyramidal neurons. (*A*) Apamin (50 nM) reduces the medium (filled arrowhead) AHP, but not the slow AHP (open arrowhead), which is instead suppressed by 100 μM 8CPT-cAMP. The AHP was elicited by a spike burst in response to a 400-ms depolarizing current pulse generating always the same number of action potentials. Averages of five traces are shown. (*B*) Apamin (50 nM) produces an increase in the early firing frequency, without affecting spike frequency adaptation. 8CPT-cAMP instead suppresses adaptation. Same cell as in *A*. The depolarizing current pulses were 800 ms long and of constant strength. Membrane potential: −57 mV in *A* and *B*. (*C*) Action potentials evoked by a 100-ms current injection. Apamin (50 nM) modified the interspike trajectory and decreased the interval between second and third spike, as shown by the superimposed traces (*Right*). The reduction of medium AHP is also evident. Membrane potential: −55 mV. (*D*) Application of 8CPT-cAMP (100 μM) suppresses spike frequency adaptation. Addition of apamin (50 nM) causes a further reduction in the interspike intervals, suggesting that the apamin-sensitive AHP contributes to determine the firing rate. (*E*) Plot of the firing frequency at different interspike intervals for the cell displayed in *D*. The control (○) shows strong adaptation. 8CPT-cAMP (100 μM; ■) suppresses spike frequency adaptation and increases the number of spikes produced in response to the same stimulus strength. Apamin (50 nM; ●) further increases the instantaneous firing frequency, with a stronger effect on the first intervals. Depolarizing pulses: 70 pA, 800 ms. Membrane potential: −57 mV in *D* and *E*.

the number and initial frequency of action potentials elicited both by short (400-ms; not shown) and long (800-ms; Fig. 5*B*) current pulses of different amplitudes ($n = 4$), but had no effect on spike frequency adaptation ($n = 4$). sAHP and spike frequency adaptation were instead fully suppressed by the subsequent application of 8CPT-cAMP (Fig. 5 *A* and *B Right*; $n = 4$). Fig. 5*C* shows how apamin (50 nM) shortens the interspike intervals in a short burst of action potentials ($n = 4$), suggesting a role of the apamin-sensitive AHP in controlling the early frequency of firing. When the slow apamin-insensitive AHP was suppressed by 8CPT-cAMP, further addition of apamin produced an increase in the firing frequency (Fig. 5*D*) by affecting the extent of membrane repolarization during each interspike interval. This effect of apamin on the instantaneous firing frequency after the suppression of sAHP by 8CPT-cAMP is shown in Fig. 5*E*. Thus, the kinetics of I_{AHP} seem best suited to underlie the mAHP, together with I_M and I_C, and to affect the instantaneous firing rate, contributing to set the duration of the interval between action potentials in a train, rather than affecting long-term changes of firing rate such as slow adaptation in CA1 pyramidal neurons, similarly to what has been observed in neocortical Betz cells (3).

The main conclusion of this study is that CA1 pyramidal neurons express an apamin-sensitive Ca^{2+}-activated K^+ current, I_{AHP}, kinetically and pharmacologically distinct from the well characterized sI_{AHP} and contributing to the generation of the medium AHP and to the regulation of their firing properties. This result is supported by our *in situ* hybridization data, indicating that the apamin-sensitive SK subunits, SK2 and SK3, are expressed in hippocampal pyramidal neurons. These findings finally provide a molecular and electrophysiological correlate to the high density of apamin-binding sites found in the CA1 region by biochemical and histochemical methods (9, 10).

The different pharmacological features of I_{AHP} and sI_{AHP} might reflect the formation of different populations of homo- and heteromultimeric SK channels in hippocampal pyramidal neurons, since it was shown that cloned SK1 and SK2 subunits can form heteromultimeric channels with an intermediate

sensitivity to apamin compared with homomeric apamin-sensitive SK2 or apamin-insensitive SK1 channels in heterologous expression systems (32). The different kinetics of I_{AHP} and sI_{AHP} are most likely not due to different subunit compositions of the underlying SK channels, because all cloned SK channels characterized so far present a fast activation upon binding of Ca^{2+} to constitutively associated calmodulin (33). The faster time course of I_{AHP} might be closely related to the time course of the intracellular Ca^{2+} change occurring during one or more action potentials (6, 29, 34), whereas the slow kinetics of sI_{AHP} might be due to mobilization of Ca^{2+} from intracellular stores (6), diffusion of Ca^{2+} to the sAHP channels from remote sites of entry (19, 35), or to delayed facilitation of L-type Ca^{2+} channels (36). In a recent interesting study, a functional coupling has been proposed between SK channels and L-type calcium channels in hippocampal neurons (37). Our results add another level of complexity to that study, posing the question whether the characterized channels belonged to the apamin-sensitive or -insensitive type. More experiments are needed to clarify whether SK channels underlying these currents are functionally coupled with different sources of Ca^{2+} in CA1 pyramidal neurons.

Two recent reports (38, 39) have presented evidence that apamin facilitates synaptic enhancement or long-term potentiation in aged or adult rats. Furthermore, there is evidence that application of apamin *in vivo* improves learning and memory retention in rats (40, 41). Taken together with our results, these findings open a number of questions on the possible role of apamin-sensitive SK channels in modulating the integration of synaptic signals in hippocampal pyramidal neurons.

We are very grateful to Walter Stühmer for generous support. We thank Lia Forti and Daniel Kerschensteiner for critically reading the manuscript; Christine Karschin for advice on the *in situ* hybridization experiments; Michael Hörner for help with the photos; and Ralf Schliephacke and Reiner Schubert for technical assistance. This work has been performed in the framework of the SFB406, project C8. M.K. is enrolled in a graduate program at the University of Düsseldorf. P.P. acknowledges support from a Human Frontier Science Program Long-Term Fellowship and a Rotary Foundation Ambassadorial Scholarship.

1. Lancaster, B. & Adams, P. R. (1986) *J. Neurophysiol.* **55,** 1268–1282.
2. Constanti, A. & Sim, J. A. (1987) *J. Physiol. (London)* **387,** 173–194.
3. Schwindt, P. C., Spain, W. J., Foehring, R. C., Stafstrom, C. E., Chubb, M. C. & Crill, W. E. (1988) *J. Neurophysiol.* **59,** 424–449.
4. Storm, J. F. (1990) *Prog. Brain Res.* **83,** 161–187.
5. Sah, P. (1996) *Trends Neurosci.* **19,** 150–154.
6. Sah, P. & McLachlan, E. M. (1991) *Neuron* **7,** 257–264.
7. Storm, J. F. (1989) *J. Physiol. (London)* **409,** 171–190.
8. Zhang, L. & McBain, C. J. (1995) *J. Physiol. (London)* **488,** 661–672.
9. Mourre, C., Hugues, M. & Lazdunski, M. (1986) *Brain Res.* **382,** 239–249.
10. Gehlert, D. R. & Gackenheimer, S. L. (1993) *Neuroscience* **52,** 191–205.
11. Köhler, M., Hirschberg, B., Bond, C. T., Kinzie, J. M., Marrion, N. V., Maylie, J. & Adelman, J. P. (1996) *Science* **273,** 1709–1714.
12. Wisden, W. & Morris, B. J. (1994) in *In Situ Hybridization Protocols for the Brain,* eds. Wisden, W. & Morris, B. J. (Academic, London), pp. 9–34.
13. Paxinos, G. & Watson, C. (1986) *The Rat Brain in Stereotaxic Coordinates* (Academic, San Diego).
14. Pedarzani, P. & Storm, J. F. (1993) *Neuron* **11,** 1023–1035.
15. Blanton, M. G., Lo Turco, J. J. & Kriegstein, A. R. (1989) *J. Neurosci. Methods* **30,** 203–210.
16. Johnson, S. W. & Seutin, V. (1997) *Neurosci. Lett.* **231,** 13–16.
17. Seutin, V., Scuvee Moreau, J. & Dreese, A. (1997) *Neuropharmacology* **36,** 1653–1657.
18. Debarbieux, F., Brunton, J. & Charpak, S. (1998) *J. Neurophysiol.* **79,** 2911–2918.
19. Lancaster, B. & Zucker, R. S. (1994) *J. Physiol. (London)* **475,** 229–239.
20. Castle, N. A. & Strong, P. N. (1986) *FEBS Lett.* **209,** 117–121.
21. Chicchi, G. G., Gimenez Gallego, G., Ber, E., Garcia, M. L., Winquist, R. & Cascieri, M. A. (1988) *J. Biol. Chem.* **263,** 10192–10197.
22. Auguste, P., Hugues, M., Grave, B., Gesquiere, J. C., Maes, P., Tartar, A., Romey, G., Schweitz, H. & Lazdunski, M. (1990) *J. Biol. Chem.* **265,** 4753–4759.
23. Auguste, P., Hugues, M., Mourre, C., Moinier, D., Tartar, A. & Lazdunski, M. (1992) *Biochemistry* **31,** 648–654.
24. Nohmi, M. & Kuba, K. (1984) *Brain Res.* **301,** 146–148.
25. Cook, N. S. & Haylett, D. G. (1985) *J. Physiol. (London)* **358,** 373–394.
26. Dun, N. J., Jiang, Z. G. & Mo, N. (1986) *J. Physiol. (London)* **375,** 499–514.
27. Bourque, C. W. & Brown, D. A. (1987) *Neurosci. Lett.* **82,** 185–190.
28. Nicoll, R. A., Malenka, R. C. & Kauer, J. A. (1990) *Physiol. Rev.* **70,** 513–565.
29. Schwindt, P. C., Spain, W. J. & Crill, W. E. (1992) *J. Neurophysiol.* **67,** 216–226.
30. Storm, J. F. (1987) *J. Physiol. (London)* **385,** 733–759.
31. Caeser, M., Brown, D. A., Gähwiler, B. H. & Knöpfel, T. (1993) *Eur. J. Neurosci.* **5,** 560–569.
32. Ishii, T. M., Maylie, J. & Adelman, J. P. (1997) *J. Biol. Chem.* **272,** 23195–23200.
33. Xia, X. M., Fakler, B., Rivard, A., Wayman, G., Johnsonpais, T., Keen, J. E., Ishii, T., Hirschberg, B., Bond, C. T., Lutsenko, S., Maylie, J. & Adelman, J. P. (1998) *Nature (London)* **395,** 503–507.
34. Lasser-Ross, N., Ross, W. N. & Yarom, Y. (1997) *J. Neurophysiol.* **78,** 825–834.
35. Zhang, L., Pennefather, P., Velumian, A. A., Tymianski, M., Charlton, M. & Carlen, P. L. (1995) *J. Neurophysiol.* **74,** 2225–2241.
36. Cloues, R. K., Tavalin, S. J. & Marrion, N. V. (1997) *J. Neurosci.* **17,** 6493–6503.
37. Marrion, N. V. & Tavalin, S. J. (1998) *Nature (London)* **395,** 900–905.
38. Norris, C. M., Halpain, S. & Foster, T. C. (1998) *J. Neurosci.* **18,** 3171–3179.
39. Behnisch, T. & Reymann, K. G. (1998) *Neurosci. Lett.* **253,** 91–94.
40. Messier, C., Mourre, C., Bontempi, B., Sif, J., Lazdunski, M. & Destrade, C. (1991) *Brain Res.* **551,** 322–326.
41. Deschaux, O., Bizot, J. C. & Goyffon, M. (1997) *Neurosci. Lett.* **222,** 159–162.